Response of Norwegian Sea temperature to solar forcing since 1000 A.D.

H. P. Sejrup,[1] S. J. Lehman,[2] H. Haflidason,[1] D. Noone,[3] R. Muscheler,[4] I. M. Berstad,[1] and J. T. Andrews[2]

Received 15 March 2010; revised 21 June 2010; accepted 20 August 2010; published 16 December 2010.

[1] We report on a 1000 year long oxygen isotope record in sediments of the eastern Norwegian Sea which, we argue, represents the temperature and transport of warm Atlantic waters entering the Nordic Sea basin via the North Atlantic Drift and the large-scale Meridional Overturning Circulation. The single-sample resolution of the record is 2.5–10 years and age control is provided by ^{210}Pb and ^{137}Cs dating, identification of historic tephra, and a ^{14}C "wiggle-match" dating method in which the surface reservoir ^{14}C age in the past is constrained rather than assumed, thereby eliminating a large source of chronological uncertainty. The oxygen isotope results indicate decade- to century-scale temperature variations of 1–2°C in the shallow (~50 m deep) subsurface which we find to be strongly correlated with various proxies of past solar activity. The correlations are synchronous to within the timescale uncertainties of the ocean and solar proxy records, which vary among the records and in time with a range of about 5–30 years. The observed ocean temperature response is larger than expected based on simple thermodynamic considerations, indicating that there is dynamical response of the high-latitude ocean to the Sun. Correlations of our results with a gridded temperature reconstruction for Europe are greater in central Europe than in coastal regions, suggesting that the temperature and transport of warm Atlantic waters entering the Nordic Basin and the pattern of temperature variability over Europe are both the proximate responses to a change in the atmospheric circulation, consistent with a forced shift in the primary modes of high-latitude atmospheric variability.

Citation: Sejrup, H. P., S. J. Lehman, H. Haflidason, D. Noone, R. Muscheler, I. M. Berstad, and J. T. Andrews (2010), Response of Norwegian Sea temperature to solar forcing since 1000 A.D., *J. Geophys. Res.*, *115*, C12034, doi:10.1029/2010JC006264.

1. Introduction

[2] The proxy record of solar variability from cosmogenic nuclides and telescopic observations of sunspots explains a substantial fraction of reconstructed Northern Hemisphere temperature variability during the pre-Industrial portion of the last millennium [e.g., *Mann et al.*, 1998], with a simulated range of up to 0.4°C for plausible irradiance scaling and climate sensitivity [*Crowley*, 2000; *Ammann et al.*, 2007]. In the satellite era, the variation in Total Solar Irradiance (TSI) during recent ~11 year "sun spot" cycles has been 0.08–0.1%, with a global average surface temperature response of 0.1 to 0.2°C [*Lean et al.*, 2005]. At both the intra- and supradecadal timescales there appear to be regional responses to solar forcing that are significantly larger than the global or hemisphere-scale response [*Woods and Lean*, 2007; *Tung and Camp*, 2008; *Shindell et al.*, 2001], suggesting that solar variations influence the atmospheric dynamics in addition to the planetary energy balance. The dynamical response may also be expected to include the ocean [cf. *White et al.*, 1998; *Mann et al.*, 2005], but the evidence of a sustained solar influence on ocean temperature and circulation at high latitudes remains in question [*Bond et al.*, 2001; *Turney et al.*, 2005; *Andrews et al.*, 2009]. Here we present an exceptionally well-dated marine sediment sequence in the eastern Norwegian Sea which records 1–2°C variations of temperature in northward flowing Atlantic waters that are robustly correlated with various estimates of solar activity spanning the last 1000 years. The temperature and solar proxy variations appear to be synchronous within dating errors, which, together with the large amplitude of the temperature signal and its correlation into central Europe, suggests strong coupling of the regional atmospheric and oceanic responses to the Sun. We surmise that this may arise from a forced shift in one or more modes of the high-latitude atmospheric

[1]Department of Earth Science, University of Bergen, Bergen, Norway.
[2]Institute of Arctic and Alpine Research, University of Colorado at Boulder, Boulder, Colorado, USA.
[3]Department of Atmospheric and Oceanic Sciences and Cooperative Institute for Research in Environmental Sciences, University of Colorado at Boulder, Boulder, Colorado, USA.
[4]GeoBiosphere Science Centre, Lund University, Lund, Sweden.

0148-0227/10/2010JC006264

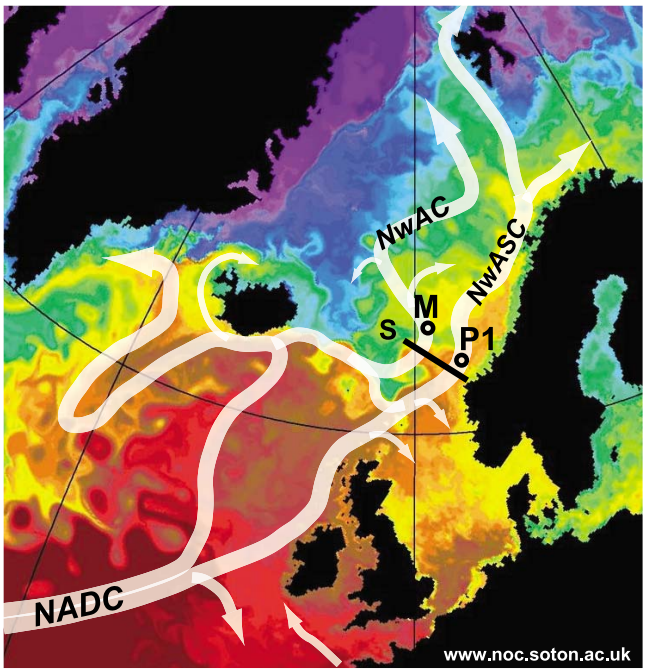

Figure 1. Main warm water surface flows of the northern North Atlantic and Nordic Sea basin, along with the locations of sediment cores P1-003MC and P1-003SC (P1), Ocean Weather Station Mike (M [*Østerhus et al.*, 1996]), and the Svinøy hydrographic section (S [*Orvik et al.*, 2001]). The labels "NwAC," "NwASC," and "NADC" refer to the Norwegian Atlantic, Norwegian Atlantic Slope, and North Atlantic Drift currents, respectively [*Orvik and Niiler*, 2002]. Underlying advanced Very High Resolution Radiometer image is for summer from the National Oceanography Centre, Southampton.

variability [cf. *Shindell et al.*, 2001] that, in turn, influence the transport of warm Atlantic water into the eastern Norwegian Sea.

2. Materials, Setting, and Methods

[3] Our results come from paired sediment cores (multicore P1-003MC and piston core P1-003SC) located beneath the axis of the warm Norwegian Atlantic Slope Current (NwASC) in the eastern Norwegian Sea (Figure 1). The core sites lie within the Storegga trough, formed by a large submarine landslide that traversed the continental slope ~8200 years B.P., creating a bathymetric catchment for subsequent sediment infill of up 25 m in thickness [*Sejrup et al.*, 2004; *Haflidason et al.*, 2004]. Recent rates of sedimentation within the slide area are thus up to several millimeters per year, providing for resolution of 2.5–10 years in single 0.5 cm to 1.0 cm thick samples.

[4] The NwASC enters the Nordic Sea basin through the Faroe-Shetland Channel and its counterpart, the Norwegian Sea Atlantic Current (NwAC), enters the basin east of Iceland (Figure 1). Together they comprise both the poleward extension of the North Atlantic Drift Current and the northern limb of the large-scale Meriodional Overturning Circulation (MOC). Locally the two branches of the Atlantic inflow are relatively close together and appear in hydrographic sections as an approximately 500 m thick, 200 km wide near-surface slab of warm (>5°C) and saline (>35 practical salinity units) water [*Orvik et al.*, 2001]. The Atlantic waters constitute the principle reservoir of heat within the Nordic Sea basin, influencing Sea Surface Temperature (SST), sea-air heat fluxes, and atmospheric temperatures over a broad region. The local interannual variability of temperature within the Atlantic waters is well explained by observed changes in their volume transport, and both are apparently related to the index state of the North Atlantic Oscillation (NAO) [*Orvik et al.*, 2001]. Maximum correlations are for summertime volume transport at the Svinøy section (located in Figure 1) and average late winter/early spring (February–March–April) NAO index ($R = 0.75$ for the period 1976–1996 A.D. [*Mork and Blindheim*, 2000]), suggesting that it is the anomalous wind stress at the time of year when the NAO is most active that determines the transport [*Orvik and Skagseth*, 2003; *Skagseth et al.*, 2004].

[5] Age control for the youngest 003MC sediments is from ^{210}Pb and ^{137}Cs dating back to ~1850 A.D., as presented previously by *Berstad et al.* [2003], and identification of historic tephra erupted in 1947 A.D. ("Hekla"), 1918 A.D. ("Katla") and 1875 A.D. ("Askja") based on methods described by *Haflidason et al.* [2000]. The agreement between Pb model ages and historic tephra dates is 7–11 years (for Hekla 1947), 0–3 years (for Katla 1918), and 1–12 years (for Askja 1875), with the stated ranges deriving from the stratigraphic thickness of levels at which peak ash shard abundances were measured. Dating of the 003MC sediments from ~1695 A.D. to ~1875 A.D., and of the 003SC sediments from the core top to ~1000 A.D., is based on a ^{14}C "wiggle-match" method adapted from *Pearson* [1986], as described below. The oldest 003MC sediments (which overlap the more rapidly deposited 003SC sediments) were only sparsely dated using conventional marine calibration of ^{14}C ages [*Hughen et al.*, 2004], but with the surface ocean reservoir age determined by the wiggle-match method. The complete 003MC sediment age model was constructed by polynomial fit to the ^{210}Pb-^{137}Cs age model after 1900 A.D., the wiggle-match dates, and the conventionally calibrated ages. The age models for both cores and associated age controls are shown in Figure 2a and tabulated in the auxiliary material (Tables S1 and S2).[1]

[6] The ^{14}C wiggle-match method has been used previously to construct extended chronologies in wood [*Pearson*, 1986] and for precise calendrical dating of uniformly deposited peat sequences on land [e.g., *Kilian et al.*, 1995]. In our application, we seek to optimize the match of measured ^{14}C age of planktonic foraminifera versus sediment depth with ^{14}C age versus calendar age anomalies in the MARINE04 calibration model [*Hughen et al.*, 2004] that has been derived previously from the INTCAL04 ^{14}C calibration based, in the Holocene, on tree rings. The primary methodological assumption is that both the sedimentation rate and any local deviation of the marine mixed layer ^{14}C age from the global average MARINE04 model value (hereafter expressed as ΔR [*Stuiver et al.*, 1986]) are constant over the interval of the wiggle match. The optimal match is therefore determined by a process of stepwise adjustment of the linear sediment depth scale in order to obtain a minimum in the root mean square deviation of the measured ^{14}C ages (versus

[1] Auxiliary materials are available in the HTML. doi:10.1029/2010JC006264.

depth) from the modeled MARINE04 value (versus calendar age), analogous to the method of *Pearson* [1986]. Any remaining mean offset between the measured ^{14}C ages and the MARINE04 model ^{14}C age is then used to determine ΔR. Wiggle matches for both studied cores are given in Figure 3, where the sediment age model is determined by the relationship between horizontal depth and calendar age axes, and ΔR is the offset between the vertical axes corresponding to the measured planktonic ^{14}C ages and the MARINE04 model ^{14}C age. In a separate manuscript we describe a computationally efficient method for the objective determination of the optimal wiggle-match values of core top calendar age and sedimentation rate (which together describe the linear age-depth model) and ΔR, along with a formal description of wiggle-match dating errors. For the present work, we note that wiggle-match fit residuals for a single match spanning the last ~4000 years in the longer 003SC core (Figure 3a) are generally within the 1-sigma ^{14}C measurement errors and that ^{14}C and calendar age uncertainties are of comparable size. For the last 1000 years, the mean 1-sigma ^{14}C measurement error is ±15 years (Table S2). An advantage of the wiggle-match method over the calibration of individual ages is that intervals of little or no ^{14}C age change in the calibration relationship (so-called ^{14}C age "plateaux") that compromise conventional single-sample calibration can provide, in contrast, improved constraint of wiggle-match ages. And, most importantly in our marine application, ΔR is determined explicitly rather than assumed, eliminating an additional and potentially large source of chronological uncertainty [e.g., *Bard*, 1988].

[7] The chronology used here for piston core P1-003SC is based on a single ^{14}C wiggle match spanning the interval from 1000 A.D. to 1550 A.D. (Figure 3b), yielding the linear age-depth relationship for this core in Figure 2a. The match indicates a ΔR of 160 years prior to ~1550 A.D. (400 years B.P.). The lack of fit of the two youngest ages is, as shown below, consistent with the 003MC results which suggest an increase in ΔR after ~1550 A.D. The sedimentation rate indicated by the wiggle match for the last 1000 years is 0.097 cm/yr, similar to the long-term average rate for the last 4000 years of ~0.1 cm/yr (Figure 3a).

[8] The 003MC Pb and Cs dating indicates gradually decreasing sedimentation rate with depth (Figure 2a, the result of dewatering), so we therefore restrict the interpretation of the wiggle match for the multicore to a narrow range in order to better satisfy the methodological assumption of constant sedimentation rate. The match is anchored by the depth and age of the Askja 1875 A.D. tephra (labeled in Figure 3c), and yields age picks near the beginning and at the end of the preceding ^{14}C age plateau centered at 27 cm of ~1695 A.D. (255 years B.P.) and ~1805 A.D. (145 years

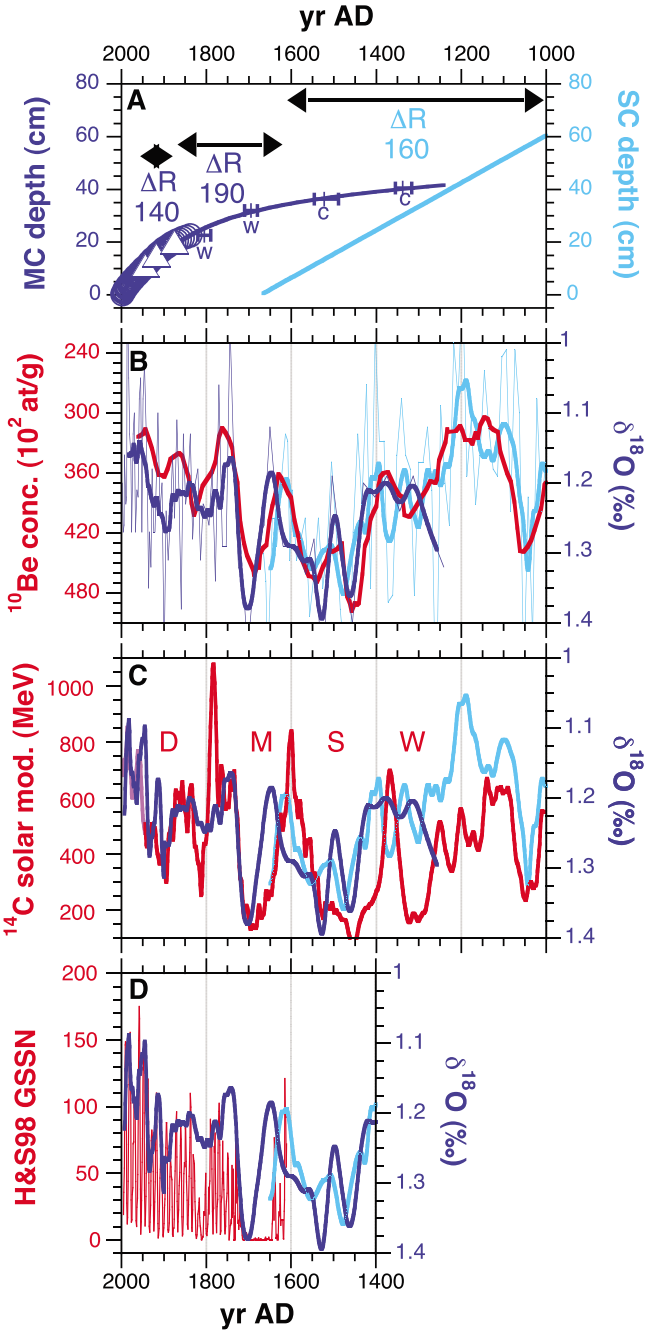

Figure 2. Sediment age models (a) for multicore P1-003MC and piston core P1-003SC based on ^{210}Pb and ^{137}Cs dating (circles), identification of historic tephra (triangles), and ^{14}C wiggle-match dating (from Figure 3), which also constrains changes in ΔR, as described in the text. P1-003MC age control points labeled "W" are from wiggle matching, and those labeled "C" are from calibration (Table S1). Also shown are raw and smoothed oxygen isotope results for 003MC and 003SC cores (light and dark blue lines, respectively) along with records of past solar activity (in red) from (b) ^{10}Be concentration in ice from South Pole, Antarctica [*Bard et al.*, 1997; *Raisbeck et al.*, 1990]; (c) solar modulation based on ^{14}C in tree rings [*Muscheler et al.*, 2007] and neutron monitor data (in purple) [*Neher*, 1967]; and (d) Group Sunspot Number [*Hoyt and Schatten*, 1998]. D, M, S, and W refer to the Dalton, Maunder, Spører, and Wolf minima, respectively. The ^{10}Be series (Figure 2a) is shown with the smoothing of ~30–40 years of *Bard et al.* [1997]. The ^{14}C-based solar modulation (Figure 2c) is shown with 11 year smoothing, and the GSSN (Figure 2d) is annual. Correlation coefficients given in the text and Table 1 are always for comparable smoothing of the solar and oxygen isotope series, which is described in the text.

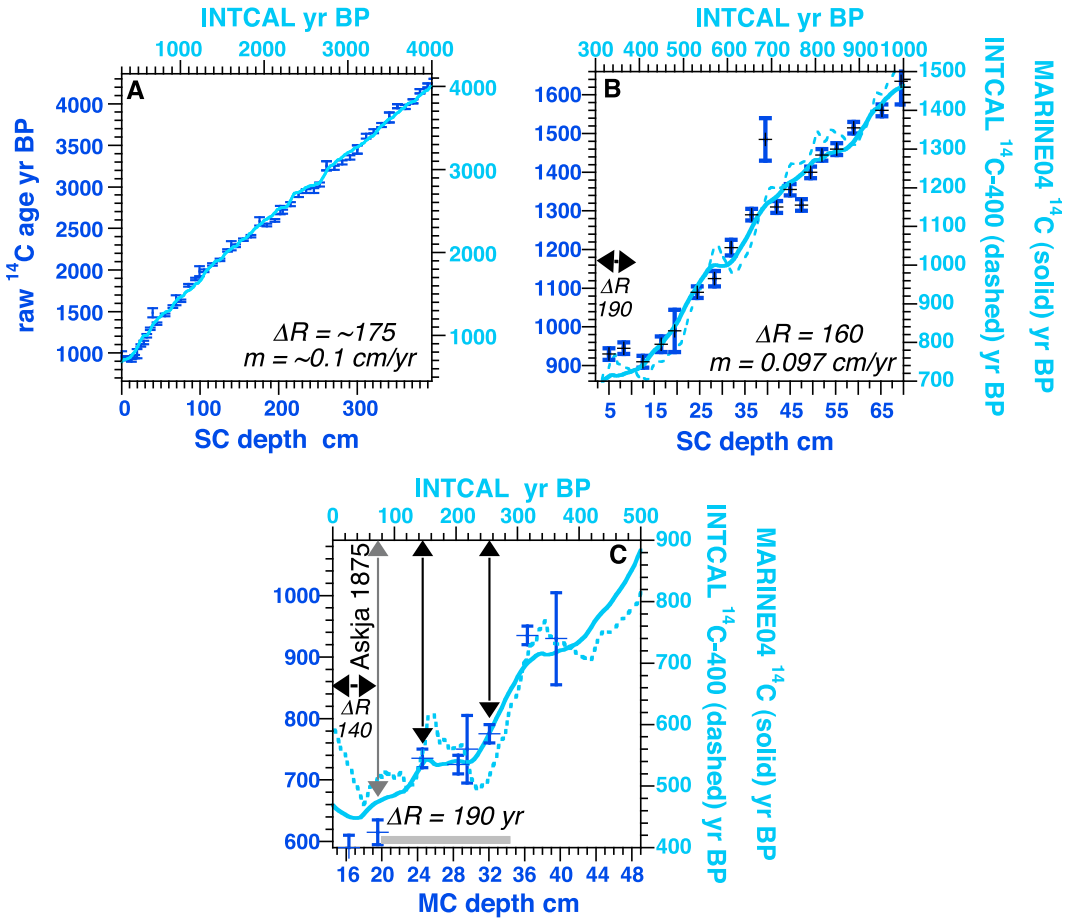

Figure 3. The ^{14}C wiggle matches for cores P1-003MC and P1-003SC. The match seeks to obtain a fit between down core measurements of ^{14}C age in planktonic foraminifera (dark blue symbols) and the MARINE04 global ocean mixed layer model (light blue solid curves). The latter is derived from the INTCAL04 calibration relationship between the ^{14}C age and calendar age of tree rings (light blue dashed curves). The ^{14}C age axes for a given match have the same range so that the local deviation of marine ^{14}C results from the MARINE04 global mixed layer age (ΔR) is simply the offset between vertical axes. The sedimentation rate is assumed to be constant for the interval of the wiggle match and its value ("*m*") is determined by the relationship between the depth scale and calendar age scale on the horizontal axes. (a) A wiggle match for P1-003SC spanning the last ~4000 years clearly shows the structures of the MARINE04 model curve. (b) A shorter wiggle-match window is used to constrain the chronology of P1-003SC after 1000 A.D. for the present study. (c) The 003MC wiggle match is valid only for the interval between 19 and 33 cm (gray bar) and is anchored by the age and depth of the oldest of the historic tephra, deposited in 1875 A.D. ("Askja"). The ^{14}C results in the youngest part of the 003SC record in Figure 3b indicate a change in ΔR after ~350 calendar years B.P. (~1600 A.D.) to the value implied by the 003MC wiggle match in Figure 3c. The error bars are 1-sigma. The ^{14}C results are from the University of Colorado at Boulder/University of California Irvine, with the exception of measurements with larger errors which are from other laboratories (Tables S1 and S2).

B.P.). The associated ΔR is 190 years prior to ~1850 A.D. (100 years B.P.). This compares to an average ΔR of 140 ± 20 years determined by ^{14}C dating planktonic foraminifera that were sampled close to the 1918 A.D. and 1875 A.D. tephras (within 1.2 cm and 0.5 cm, respectively). The position of the corresponding ^{14}C ages (at 15 and 19 cm depth in Figure 3c) ~50 years below the wiggle match for the older 003MC ages is consistent with a change in ΔR to ~140 years sometime between ~1805 A.D. and 1875 A.D. This value is within the range of previous estimates of ΔR from coastal mollusks in the Norwegian Sea for the late 19th and early 20th centuries [*Mangerud et al.*, 2006, Figure 2].

[9] Our climate reconstruction is based on measurements of $\delta^{18}O$ in *Neogloboquadrina pachyderma* (dextral form), a planktonic foraminifer that calcifies at relatively shallow depths within the Atlantic waters of the eastern Norwegian Sea during late summer [*Johannessen et al.*, 1994; *Berstad et al.*, 2003; *Nyland et al.*, 2006]. In order to evaluate the extent to which down core variations in *N. pachyderma* (dex.) $\delta^{18}O$ reflect the temperature of these Atlantic waters, we compare (Figure 4 (top)) down core isotope results on the

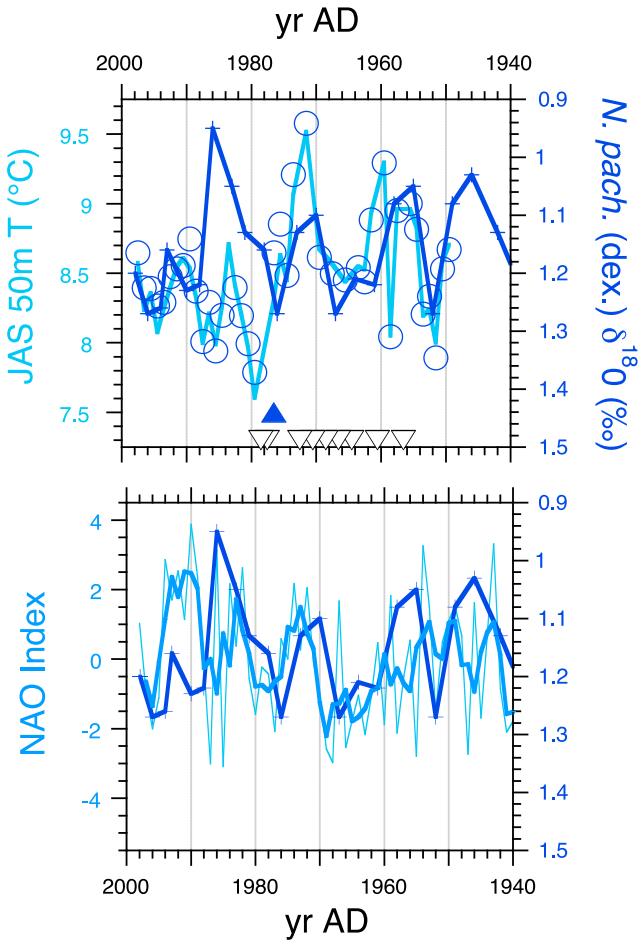

Figure 4. Comparison of P1-003MC isotope results with hydrographic observations and the annual NAO index. (top) P1-003MC *N. pachyderma* (dex.) $\delta^{18}O$ on the ^{210}Pb and ^{137}Cs age model (Table S1) and ocean temperatures for the approximate season and depth of *N. pachyderma* (dex.) calcification. Temperatures are annual averages for July–August–September (JAS) from 50 m depth at Ocean Weather Station Mike (OWSM, located in Figure 1). Temperature and isotope axes are scaled according to the relationship expected for temperature-dependent isotope fractionation between seawater and calcite (~−0.25°C/‰ at low temperatures [*Shackleton*, 1974]). Estimates of equilibrium calcite $\delta^{18}O$ values for 50 m JAS temperature and salinity pairs from OWSM (dark blue circles) have been corrected arbitrarily by −1.09 ‰ for presentation on the *N. pachdyderma* (dex.) scale. Missing years in the hydrographic observations are identified by open triangles on the horizontal axis. The blue triangle marks the coldest July of the record, which corresponds with a $\delta^{18}O$ maximum (isotopic cooling) at the beginning of the interval of proxy temperature mismatch discussed in the text. The average single-sample resolution of the sediment record across the interval of comparison with the hydrographic data is 2.5 years. (bottom) *N. pachyderma* (dex.) $\delta^{18}O$ as in Figure 4a and the annual NAO index with (thick line) and without (thin line) 3 year smoothing, which has been applied to approximate the resolution of the sediment record. The NAO index is from the Climate Analysis Section, NCAR, Boulder, United States [*Hurrell*, 1995].

003MC Pb-Cs age model with hydrographic observations available since 1950 A.D. from Ocean Weather Station Mike (OWSM, at 66°N, 2°E), located approximately 200 km north of the core sites and within the NwAC (Figure 1). Temperatures in Figure 4 (top) are yearly averages for July–August–September (JAS) from 50 m depth, and temperature and isotope axes are scaled according to the relationship expected for temperature-dependent isotope fractionation between seawater and calcite (i.e., approximately −0.25‰/°C based on the linear approximation of the ($\delta^{18}O_{calcite}$-$\delta^{18}O_{water}$):T relationship at low temperatures of *Shackleton* [1974]). The range of measured *N. pachyderma* (dex.) $\delta^{18}O$ is comparable to that expected due to the observed temperature changes and many of the features of the $\delta^{18}O$ and temperature series are shared. There is, however, a conspicuous scale (but not amplitude) offset in the mid-1970s to mid-1980s that may be due to atypical development of the summer season in that period, which contains the coldest July (1976, blue triangle in Figure 4 (top)) and some of the warmest Septembers of the record (individual summer monthly temperatures are given in Figure S1). Thus, 3 month JAS averages may be less representative of the range of possible short-term growth temperatures during this interval. In order to estimate the possible contribution of salinity changes to the isotope signal, we calculated equilibrium calcite $\delta^{18}O$ values for 50 m JAS temperature and salinity pairs from OWSM using a salinity versus $\delta^{18}O_{water}$ relationship for the Atlantic from *Ostlund et al.* [1987] and the linear "paleotemperature" equation of *Shackleton* [1974] just mentioned. The calculated values have been corrected arbitrarily by −1.09 ‰ for presentation on the *N. pachdyderma* (dex.) scale (open circles in Figure 4 (top)) and indicate that, at least since 1950 A.D., the influence of salinity on the expected isotope signal has been negligible. Differences between the *N. pachyderma* (dex.) $\delta^{18}O$ and temperature series are most likely due to variable smoothing by the sediment record (with a mean resolution of 2.5 years in this interval), variations in the weighted mean timing and depth of *N. pachyderma* (dex.) calcification, uncertainties of the Pb and Cs age model and, possibly, authentic differences between hydrographic variation at OWSM (in the NwAC) and at the core site (in the NwASC). Due to the complications of reconstructing absolute isotope paleotemperature [cf. *Nyland et al.*, 2006] we restrict our interpretation to a discussion of relative temperature variation. To do this we apply a scaling of −0.25 ‰/°C, which is at the high sensitivity end of available calibrations (which are otherwise for warm water [cf. *Bemis et al.*, 1998]). This can be expected to yield relatively conservative isotopic estimates of temperature change. Because *N. pachyderma* (dex.) calcify in the shallow subsurface, we will refer to reconstructed temperatures as variations of near SST or nSST.

3. Results

[10] Raw and temporally smoothed $\delta^{18}O$ results for both cores are given in Figure 2b. We applied both 11 and 30 year smoothing to the $\delta^{18}O$ data of the last 100 years (Figure 2b versus Figures 2c and 2d, respectively) in order to permit comparison with solar proxy records of different resolution. For the older parts of the series, where the single sample resolution is 7–10 years, we apply a 30 year

Table 1. Correlation *R* Between the Oxygen Isotopic Series and Various Solar Proxy Reconstructions[a]

P1-003MC/SC δ^{18}O Compared to	Complete Series	From 1500 A.D. Only
Bard smoothed South Pole ^{10}Be concentration	0.79 (32)	0.87 (15)
11 year/30 year smoothed ^{14}C-based Phi	−0.54 (37)	−0.71 (21)
30 year smoothed ^{14}C-based Phi	−0.54 (31)	−0.71 (15)
11 year/30 year smoothed GSSN		−0.80 (17, from 1625)
30 year smoothed GSSN		−0.80 (11, from 1625)

[a]Phi, solar modulation factor; GSSN, Group Sun Spot Number. Estimated number of degrees of freedom is given in parentheses. All correlations are significant at the >99% level. The marine isotope record has been subjected to 30 year smoothing, except for the comparison to the better resolved and dated ^{14}C-based and GSSN reconstructions, where the smoothing is 11 years after 1900 A.D., as explained in the text. The solar series are smoothed in the same way as the oxygen isotope series for all correlations.

smoothing only. The smoothed 003MC and 003SC series show similar patterns of isotopic variation for the period of overlap, suggesting that the reconstructions are robust despite differences in sedimentation rate and sample resolution between cores. Lowest isotope values (highest temperatures) of the last millennium are seen ~1100–1300 A.D., during the Medieval Climate Anomaly [*Bradley et al.*, 2003], and again after ~1950 A.D. The largest and most sustained isotopic increases (coolings) are centered at ~1500 A.D. and ~1700 A.D., corresponding to the regional Little Ice Age [*Jones and Bradley*, 1992]. Isotopic increases at these times are ~0.3 ‰, indicating decreases of nSST of 1–1.5°C. After smoothing, the amplitude of nSST change over the last millennium is 1.5–2°C.

[11] The presence of medieval and 20th century warmth and Little Ice Age cooling in our records suggests a possible connection to known solar variations at these times (i.e., the Spører and Maunder minima and medieval and modern maxima, respectively [*Eddy*, 1976; *Frohlich and Lean*, 2002]). In Figures 2b–2d we compare the Norwegian Sea results directly with proxies of solar variability that span all or part of the last millennium on their independently derived age scales. These include changes in ^{10}Be concentration in ice from South Pole, Antarctica [*Bard et al.*, 1997; *Raisbeck et al.*, 1990] (Figure 2b), an estimate of cosmic ray modulation by the Sun's open magnetic flux based on Δ^{14}C variations in tree rings [*Muscheler et al.*, 2007] (Figure 2c), and telescopic observations of Group Sunspot Number (GSSN) since 1610 A.D. [*Hoyt and Schatten*, 1998] (Figure 2d). Absolute values of the correlation of Norwegian Sea isotope results with the ^{10}Be- and ^{14}C-based solar proxies are 0.79 and 0.54, respectively, and both are significant at the 99% level (Table 1). For the period after 1500 A.D., during which we have greatest confidence in the sediment age model, correlations with the various solar proxies range from $|R|$ = 0.71 to 0.87 (all significant at >99%). The weaker correlation of the complete δ^{18}O record with the ^{14}C-based solar series arises primarily from the large amplitude variability in the solar proxy between 1300 and 1450 A.D. that is not seen in the temperature proxy (Figure 2c).

[12] Similarity in both timing and amplitude of 30 year smoothed δ^{18}O and South Pole ^{10}Be series in Figure 2b suggest an approximately linear response of near-surface temperature in the eastern Norwegian Sea to solar variations of the last millennium. (The alternative interpretation of changes in the mechanism of ^{10}Be deposition at the South Pole that are linear in North Atlantic climate is highly unlikely). The δ^{18}O-^{10}Be relationship is on average synchronous to within a timescale determined by the resolution and the nonstationary age uncertainties of the individual records of up to ~30 years (Figure S2). After ~1800 A.D., δ^{18}O appears to lead South Pole ^{10}Be (Figure 2b), whereas the comparison with the better resolved and better dated ^{14}C- and GSSN-based solar proxies (Figures 2c and 2d) indicates a relationship that is synchronous. In contrast to the South Pole ^{10}Be versus δ^{18}O relationship, the first and second halves of the ^{14}C-based solar series show significant differences in amplitude scaling with respect to δ^{18}O. This may be due in part to a change in resolution of the INTCAL Δ^{14}C record, from which the ^{14}C-based solar reconstruction has been derived, from decadal to annual at 1500 A.D. In addition, this may be the result of a change in the ocean circulation that has influenced the partitioning of ^{14}C between the deep ocean and atmosphere.

[13] On balance, the observed relationship of nSST and solar proxies suggests a climate response to the Sun within the characteristic inertial timescale of the upper ocean, which is one to several decades [*Stouffer*, 2004]. Recurrent, episodic volcanic forcing may also influence the ocean climate signal at this timescale [*Weber*, 2005], however, our results indicate that approximately 50–70% of the observed multidecadal to century-scale δ^{18}O variation may be explained by solar forcing alone.

4. Discussion

[14] Despite uncertainty in relating solar proxies to absolute variations of the TSI (or the spectral irradiance) [*Lean et al.*, 2002], it is clear that temperature changes of 1–2°C are large with respect to global or hemisphere-scale surface temperature changes expected in direct response to plausible long-term variations of the TSI in the range of 0.1 to 0.4%. The latter equate to changes in radiative forcing of 0.2 to 0.9 W/m^2 (i.e., top-of-atmosphere TSI*(1–0.3)/4), which may be expected to produce a temperature response of 0.1 to 0.5°C (given, for example, a transient climate response of ~0.5°C per W/m^2 [*Intergovernmental Panel on Climate Change*, 2007]). As simple thermodynamic considerations would lead us to expect smaller temperature changes at the ocean surface than over land, the relatively large near-surface temperature signal we document points to significant regional amplification arising from a dynamical response of the atmosphere-ocean system.

[15] The leading dynamical modes of atmospheric variability in the mid- to high latitudes of the Northern Hemisphere are the NAO and the related Arctic Oscillation (AO) (we follow *Wallace* [2000] in regarding the NAO and AO as the surface expressions of the Northern Annular Mode at different spatial scales). The states of both the NAO and AO can be defined in terms of differences in surface pressure between the Arctic and the midlatitudes, where the positive index state (negative anomaly of Arctic pressure) is associated with enhanced westerly flow of warm ocean air into

central and northern Europe and the negative index state (positive anomaly of Arctic pressure) is characterized by a weakened zonal circulation and greater penetration of Arctic air over the continent. As a result, the NAO/AO exerts a large influence on the climate of the European and North Atlantic sectors, most notably in wintertime when the large-scale atmospheric circulation is more active. A number of studies have documented the imprint of NAO/AO-like spatial patterns of temperature variability in European and Northern Hemisphere climate reconstructions spanning the last few centuries [cf. *Mann et al.*, 1998; *Slonosky et al.*, 2001; *Casty et al.*, 2007]. It also appears that these (or similar) patterns can be elicited as a forced response to solar variations in some numerical models (through a range of mechanisms [cf. *Haigh*, 1999; *Shindell et al.*, 1999, 2001; *Emile-Geay et al.*, 2007]). For example, using a General Circulation Model with an interactive stratosphere, *Shindell et al.* [2001] show a temperature response to a decrease in spectral irradiance during the Maunder minimum that is well characterized by a low index state of the model's AO/NAO. A solar influence on the regional modes of atmospheric variability is now also evident in the instrumental record [*Kodera and Kuroda*, 2002; *Ruzmaikin et al.*, 2004; *Haigh and Roscoe*, 2006].

[16] We have already noted the present-day relationship between the NAO, anomalous wind stress, and the temperature and transport of Atlantic waters in the eastern Norwegian Sea at the interannual timescale [i.e., *Mork and Blindheim*, 2000; *Orvik and Skagseth*, 2003; *Skagseth et al.*, 2004], while the correlation of δ^{18}O and solar proxies we observe over the last millennium indicates a persistent solar influence on the warm water transport at the decade to century timescale. We surmise that the latter may result from a shift in the regional modes of atmospheric variability under sustained solar forcing [cf. *Shindell et al.*, 2001], with the warm water transport responding directly to altered wind stress [cf. *Krahmann et al.*, 2001] and/or indirectly to altered buoyancy forcing of the MOC [*Delworth and Dixon*, 2000; *Eden and Willebrand*, 2001].

[17] In order to characterize the relationship between our record of Atlantic water temperature and transport and the regional climate variability in the past, we chose to calculate correlations of eastern Norwegian Sea δ^{18}O with the 0.5° × 0.5° gridded seasonal temperature reconstruction for Europe of *Luterbacher et al.* [2004], which covers the last 500 years and therefore spans several large, apparently forced nSST cycles. (Unfortunately, the lack of adequately resolved and dated marine records does not permit us to evaluate the correlation field over the ocean.) Both the sediment record and the gridded reconstruction were smoothed by 30 years prior to correlation. The instantaneous map correlation pattern for gridded annual mean temperature is shown in Figure 5a. The annual pattern is dominated by those for winter and spring (not shown), and is marked by large and significant negative δ^{18}O versus map temperature correlations (i.e., positive for ocean versus map temperature) in central Europe that diminish steeply toward Iceland and the Middle East. The fact that maximum correlations are observed in central Europe and not in Atlantic coastal areas argues against a mainly localized or "maritime" influence of the warm water transport on the pattern of regional temperature variability and instead for relatively discrete responses of both the warm water transport and the regional temperature variability to the atmospheric circulation. The lag correlation functions of Norwegian Sea δ^{18}O versus individual seasons in the gridded reconstruction are given in Figure 5b as the quadratic mean of R for all map grid points by year either before or after the sediment record. These show the largest and most immediate correlations in winter and spring when the atmospheric circulation is most vigorous and the amplitude of temperature variability in the gridded reconstruction is greatest.

[18] We next consider the relationship between the spatial correlation pattern in Figure 5a and that for late winter/early spring NAO index versus annual mean surface temperature in the instrumental period, which is given in Figure 5c. Both show pronounced zonal structures with correlation maxima extending across central Europe. The similarity of spatial correlations elicited by the sediment δ^{18}O and seasonal NAO index is thus consistent with the suggestion that both the warm water transport and the patterns of regional temperature charge were proximate responses to a forced shift in the NAO/AO-like (or, more broadly, annular) modes of variability in the past. As the regional forcing of the warm water transport in the eastern Norwegian Sea appears to be greatest in late winter/early spring, Figure 5c is a plausible physical analog for the δ^{18}O versus map temperature relationship in Figure 5a, although the timescales considered are different. We obtain a similar result for the modern correlation using the annual average annual NAO index (Figure S3).

[19] Variations in the warm water transport might also arise from a solar influence on the MOC that is independent of the NAO/AO. In the instrumental record, apparently unforced variability of the MOC is detectable as a North Atlantic basin-wide SST anomaly of common sign known as the Atlantic Multidecadal Oscillation (AMO [*Kerr*, 2000]). In contrast to those for the 003MC/SC δ^{18}O record or the NAO indices, correlations of the AMO index [*Enfield et al.*, 2001; *Sutton and Hodson*, 2005] into Europe are largest in Scandinavia and weak in central Europe (Figure 5d). We therefore suggest that the solar influence on near-surface temperatures of the eastern Norwegian Sea is exerted primarily through a dynamical response of the atmosphere, consistent with a prior analysis of the instrumental record of SST and sea level pressure at the global scale [*Lohmann et al.*, 2004].

5. Conclusions

[20] We have presented an oxygen isotopic proxy record of near-surface temperature of Atlantic waters from the area of their primary flow into the eastern Norwegian Sea and find that it is robustly and near-synchronously correlated with various proxies of solar variability spanning the last millennium. The associated decade- to century-scale variation of estimated nSST ranges from 1 to 2°C, significantly larger than expected based on thermodynamic considerations alone. We suggest that this is due to a solar influence on the regional modes of atmospheric variability which, in turn, control the poleward transport and temperature of warm Atlantic surface waters. Our findings beg the question of why such a clear connection has not been detected previously. This may be due to improved dating of our record and, in particular, our use of a ^{14}C wiggle-match dating

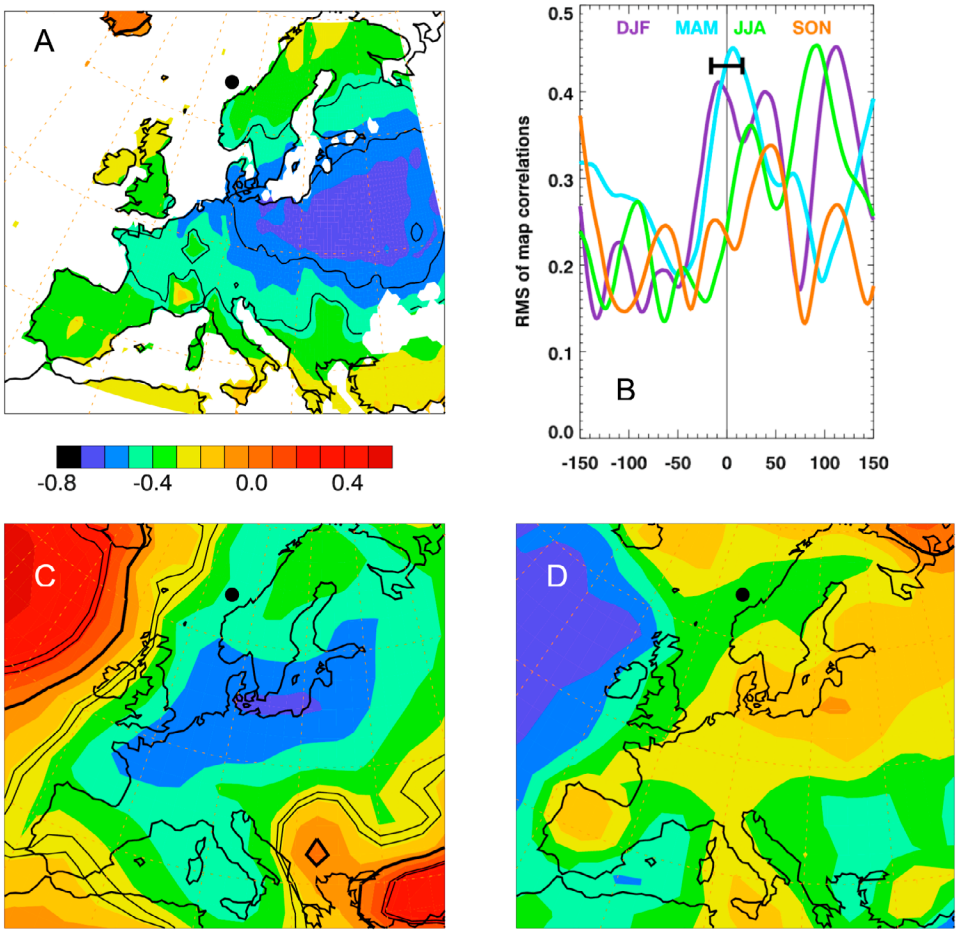

Figure 5. (a) Point correlation (R) of eastern Norwegian Sea $\delta^{18}O$ (at the location of the solid circle) with the gridded annual temperature reconstruction for Europe of *Luterbacher et al.* [2004] for the last 500 years. The area within the inner (outer) black line exceeds a significance of 95% (90%) using a two-tailed t test and accounts for autocorrelation due to smoothing. (b) Lag correlations of $\delta^{18}O$ with seasonal temperature reconstructions. The correlation is expressed as the root-mean-square (RMS) of all point correlations for a given lag year. The sediment and temperature reconstructions have been smoothed by 30 years prior to correlation. Positive lags are for map temperature following the sediment record. The resolution of the curves is limited by the smoothing (error bar), while resolution of the correlation lag is limited by variable age uncertainties of up to ~30 years, as explained in the text. Correlation of the (c) yearly February–March–April average NAO index and (d) annual average AMO index with annual average surface temperature over the domain in Figure 5a for the period 1948–2009. The modern correlations are shown with the signs reversed to permit comparison with Figure 5a and significance contours are as in Figure 5a. The significance of the AMO correlations is weak due to reduction in the number of degrees of freedom arising from autocorrelation in the index itself. The NAO index is from the Climate Analysis Section, NCAR, Boulder, United States [*Hurrell*, 1995]; the AMO index is from NOAA ESRL [*Enfield et al.*, 2001]; and temperatures are from NCEP [*Kalnay et al.*, 1996].

method in which the surface ^{14}C reservoir age in the past is constrained rather than assumed. In addition, the study site is located in an area where today the basin-scale wind forcing exerts a strong control on the local Atlantic water temperature and transport.

[21] **Acknowledgments.** H.P.S. and S.J.L. contributed equally to this work. Support for this study was provided by the Comer Science and Education Foundation (S.J.L.) and Norwegian Research Council (H.P.S. and H.H.). C. Wolak and P. Cappa assisted with ^{14}C and AMS measurements were made by John Southon. We benefited from discussions with M. K. Hughes at an early stage of this work, and J. Luterbacher kindly provided access to the gridded temperature reconstruction.

References

Ammann, C. M., F. Joos, D. S. Schimel, B. L. Otto-Bliesner, and R. A. Tomas (2007), Solar influence on climate during the past millennium: Results from transient simulations with the NCAR Climate System Model, *Proc. Natl. Acad. Sci. U. S. A.*, *104*(10), 3713–3718, doi:10.1073/pnas.0605064103.

Andrews, J. T., D. A. Darby, D. D. Eberl, A. E. Jennings, M. Moros, and A. Ogilvie (2009), A robust, multisite Holocene history of drift ice off northern Iceland: Implications for North Atlantic climate, *Holocene*, *19*, 71–77, doi:10.1177/0959683608098953.

Bard, E. (1988), Correction of accelerator mass spectrometry ^{14}C ages measured in planktonic foraminifera: Paleoceanographic implications, *Paleoceanography*, *3*(6), 635–645, doi:10.1029/PA003i006p00635.

Bard, E., G. M. Raisbeck, F. Yiou, and J. Jouzel (1997), Solar modulation of cosmogenic nuclide production over the last millennium: Comparison between ^{14}C and ^{10}Be records, *Earth Planet. Sci. Lett.*, *150*(3–4), 453–462, doi:10.1016/S0012-821X(97)00082-4.

Bemis, B. E., H. J. Spero, J. Bijma, and D. W. Lea (1998), Reevaluation of the oxygen isotopic composition of planktonic foraminifera: Experimental results and revised paleotemperature equations, *Paleoceanography*, *13*(2), 150–160, doi:10.1029/98PA00070.

Berstad, I. M., H. P. Sejrup, D. Klitgaard-Kristensen, and H. Haflidason (2003), Variability in temperature and geometry of the Norwegian Current over the past 600 yr: Stable isotope and grain size evidence from the Norwegian margin, *J. Quat. Sci.*, *18*(7), 591–602, doi:10.1002/jqs.790.

Bond, G., B. Kromer, J. Beer, R. Muscheler, M. N. Evans, W. Showers, S. Hoffman, R. Lotti-Bond, I. Hajdas, and G. Bonani (2001), Persistent solar influence on North Atlantic climate during the Holocene, *Science*, *294*(5549), 2130–2136, doi:10.1126/science.1065680.

Bradley, R. S., M. K. Hughes, and H. F. Diaz (2003), Climate in Medieval time, *Science*, *302*(5644), 404–405, doi:10.1126/science.1090372.

Casty, C., C. C. Raible, T. F. Stocker, H. Wanner, and J. Luterbacher (2007), A European pattern climatology 1766–2000, *Clim. Dyn.*, *29*(7–8), 791–805, doi:10.1007/s00382-007-0257-6.

Crowley, T. J. (2000), Causes of climate change over the past 1000 years, *Science*, *289*(5477), 270–277, doi:10.1126/science.289.5477.270.

Delworth, T. L., and K. W. Dixon (2000), Implications of the recent trend in the Arctic/North Atlantic oscillation for the North Atlantic thermohaline circulation, *J. Clim.*, *13*(21), 3721–3727, doi:10.1175/1520-0442(2000)013<3721:IOTRTI>2.0.CO;2.

Eddy, J. A. (1976), The Maunder minimum, *Science*, *192*(4245), 1189–1202, doi:10.1126/science.192.4245.1189.

Eden, C., and J. Willebrand (2001), Mechanism of interannual to decadal variability of the North Atlantic circulation, *J. Clim.*, *14*(10), 2266–2280, doi:10.1175/1520-0442(2001)014<2266:MOITDV>2.0.CO;2.

Emile-Geay, J., M. Cane, R. Seager, A. Kaplan, and P. Almasi (2007), El Niño as a mediator of the solar influence on climate, *Paleoceanography*, *22*, PA3210, doi:10.1029/2006PA001304.

Enfield, D. B., A. M. Mestas-Nunez, and P. J. Trimble (2001), The Atlantic mulitdecadal oscillation and its relation to rainfall and river flows in the continental U.S, *Geophys. Res. Lett.*, *28*(10), 2077–2080, doi:10.1029/2000GL012745.

Fröhlich, C., and J. Lean (2002), Solar irradiance variability and climate, *Astron. Nachr.*, *323*(3–4), 203–212, doi:10.1002/1521-3994(200208)323:3/4<203::AID-ASNA203>3.0.CO;2-L.

Haflidason, H., J. Eiriksson, and S. Van Kreveld (2000), The tephrochronology of Iceland and the North Atlantic region during the Middle and Late Quaternary: A review, *J. Quat. Sci.*, *15*(1), 3–22, doi:10.1002/(SICI)1099-1417(200001)15:1<3::AID-JQS530>3.0.CO;2-W.

Haflidason, H., H. P. Sejrup, A. Nygard, J. Mienert, P. Bryn, R. Lien, C. F. Forsberg, K. Berg, and D. Masson (2004), The Storegga Slide: Architecture, geometry and slide development, *Mar. Geol.*, *213*(1–4), 201–234, doi:10.1016/j.margeo.2004.10.007.

Haigh, J. D. (1999), A GCM study of climate change in response to the 11-yr solar cycle, *Q. J. R. Meterorol. Soc.*, *125*(555), 871–892, doi:10.1002/qj.49712555506.

Haigh, J. D., and H. K. Roscoe (2006), Solar influences on polar modes of variability, *Meteorol. Z.*, *15*(3), 371–378, doi:10.1127/0941-2948/2006/0123.

Hoyt, D. V., and K. H. Schatten (1998), Group sunspot numbers: A new solar activity reconstruction, *Sol. Phys.*, *179*(1), 189–219, doi:10.1023/A:1005007527816.

Hughen, K. A., et al. (2004), MARINE04 marine radiocarbon age calibration, 0–26 cal kyr BP, *Radiocarbon*, *46*(3), 1059–1086.

Hurrell, J. W. (1995), Decadal trends in the North-Atlantic Oscillation: Regional temperatures and precipitation, *Science*, *269*(5224), 676–679, doi:10.1126/science.269.5224.676.

Intergovernmental Panel on Climate Change (2007), Understanding and attributing climate change, in *Climate Change 2007: The Physical Science Basis: Working Group I Contribution to the Fourth Assessment Report of the IPCC*, edited by S. Solomon et al., pp. 663–746, Cambridge Univ. Press, New York.

Johannessen, T., E. Jansen, A. Flatøy, and A. C. Ravelo (1994), The relationship between surface water masses, oceanographic fronts and paleoclimatic proxies in surface sediments of the Greenland, Iceland, Norwegian Seas, in *Carbon Cycling in the Glacial Ocean: Constraints on the Ocean's Role in Global Change*, edited by R. Zahn et al., pp. 61–86, Springer, Berlin.

Jones, P. D., and R. S. Bradley (1992), Climatic variations over the last 500 years, in *Climate Since A.D. 1500*, edited by R. S. Bradley and P. D. Jones, pp. 649–665, Routledge, London.

Kalnay, E., et al. (1996), The NCEP/NCAR reanalysis 40-year project, *Bull. Am. Meteorol. Soc.*, *77*, 437–471, doi:10.1175/1520-0477(1996)077<0437:TNYRP>2.0.CO;2.

Kerr, R. A. (2000), A North Atlantic climate pacemaker for the centuries, *Science*, *288*(5473), 1984–1985, doi:10.1126/science.288.5473.1984.

Kilian, M. R., J. Van der Plicht, and B. Van Geel (1995), Dating raised bogs: New aspects of AMS ^{14}C wiggle matching, a reservoir effect and climatic change, *Quat. Sci. Rev.*, *14*(10), 959–966, doi:10.1016/0277-3791(95)00081-X.

Kodera, K., and Y. Kuroda (2002), Dynamical response to the solar cycle, *J. Geophys. Res.*, *107*(D24), 4749, doi:10.1029/2002JD002224.

Krahmann, G., M. Visbeck, and G. Reverdin (2001), Formation and propagation of temperature anomalies along the North Atlantic Current, *J. Phys. Oceanogr.*, *31*(5), 1287–1303, doi:10.1175/1520-0485(2001)031<1287:FAPOTA>2.0.CO;2.

Lean, J. L., Y. M. Wang, and N. R. Sheeley (2002), The effect of increasing solar activity on the Sun's total and open magnetic flux during multiple cycles: Implications for solar forcing of climate, *Geophys. Res. Lett.*, *29*(24), 2224, doi:10.1029/2002GL015880.

Lean, J., G. Rottman, J. Harder, and G. Kopp (2005), SORCE contributions to new understanding of global change and solar variability, *Sol. Phys.*, *230*(1–2), 27–53, doi:10.1007/s11207-005-1527-2.

Lohmann, G., N. Rimbu, and M. Dima (2004), Climate signature of solar irradiance variations; Analysis of long-term instrumental, historical and proxy data, *Int. J. Climatol.*, *24*, 1045–1056, doi:10.1002/joc.1054.

Luterbacher, J., D. Dietrich, E. Xoplaki, M. Grosjean, and H. Wanner (2004), European seasonal and annual temperature variability, trends, and extremes since 1500, *Science*, *303*(5663), 1499–1503, doi:10.1126/science.1093877.

Mangerud, J., S. Bondevik, S. Gulliksen, A. K. Hufthammer, and T. Hoisaeter (2006), Marine ^{14}C reservoir ages for 19th century whales and molluscs from the North Atlantic, *Quat. Sci. Rev.*, *25*(23–24), 3228–3245, doi:10.1016/j.quascirev.2006.03.010.

Mann, M. E., R. S. Bradley, and M. K. Hughes (1998), Global-scale temperature patterns and climate forcing over the past six centuries, *Nature*, *392*(6678), 779–787, doi:10.1038/33859.

Mann, M. E., M. A. Cane, S. E. Zebiak, and A. Clement (2005), Volcanic and solar forcing of the tropical Pacific over the past 1000 years, *J. Clim.*, *18*(3), 447–456, doi:10.1175/JCLI-3276.1.

Mork, M., and J. Blindheim (2000), Variations in Atlantic inflow to the Nordic Seas, 1955–1996, *Deep Sea Res. Part I*, *47*, 1035–1057, doi:10.1016/S0967-0637(99)00091-6.

Muscheler, R., F. Joos, J. Beer, S. A. Muller, M. Vonmoos, and I. Snowball (2007), Solar activity during the last 1000 yr inferred from radionuclide records, *Quat. Sci. Rev.*, *26*(1–2), 82–97, doi:10.1016/j.quascirev.2006.07.012.

Neher, H. V. (1967), Cosmic-ray particles that changed from 1954 to 1958 to 1965, *J. Geophys. Res.*, *72*(5), 1527, doi:10.1029/JZ072i005p01527.

Nyland, B. F., E. Jansen, H. Elderfield, and C. Andersson (2006), *Neogloboquadrina pachyderma* (dex. and sin.) Mg/Ca and $\delta^{18}O$ records from the Norwegian Sea, *Geochem. Geophys. Geosyst.*, *7*, Q10P17, doi:10.1029/2005GC001055.

Orvik, K. A., and P. Niiler (2002), Major pathways of Atlantic water in the northern North Atlantic and Nordic Seas toward Arctic, *Geophys. Res. Lett.*, *29*(19), 1896, doi:10.1029/2002GL015002.

Orvik, K. A., and Ø. Skagseth (2003), The impact of wind stress curl in the North Atlantic on the Alantic inflow to the Norwegian Sea toward the Arctic, *Geophys. Res. Lett.*, *30*(17), 1884, doi:10.1029/2003GL017932.

Orvik, K. A., Ø. Skagseth, and M. Mork (2001), Atlantic inflow to the Nordic Seas: Current structure and volume fluxes from moored current meters, VM-ADCP and SeaSoar-CTD observations, 1995–1999, *Deep Sea Res. Part I*, *48*, 937–957, doi:10.1016/S0967-0637(00)00038-8.

Østerhus, S., T. Gammelsrød, and R. Hogstad (1996), Ocean weather ship station M (66°N, 2°E): The longest homogeneous time series from the deep ocean, *World Ocean Circ. Exp. Newsl.*, *24*, 32–33.

Ostlund, G. H., H. Craig, W. S. Broecker, and D. W. Spencer (Eds.) (1987), *GEOSECS Atlantic, Pacific, and Indian Ocean Expeditions*, vol. 7, *Shore Based Data and Graphics*, Natl. Sci. Found., Washington, D. C.

Pearson, G. W. (1986), Precise calendrical dating of known growth-period samples using a curve fitting technique, *Radiocarbon*, *28*(2A), 292–299.

Raisbeck, G. M., F. Yiou, J. Jouzel, and J. R. Petit (1990), ^{10}Be and $\delta^{2}H$ in polar ice cores as a probe of the solar variability influence on climate, *Philos. Trans. R. Soc. London A*, *330*(1615), 463–470.

Ruzmaikin, A., J. Feynman, X. Jiang, D. C. Noone, A. M. Waple, and Y. L. Yung (2004), The pattern of northern hemisphere surface air temperature during prolonged periods of low solar output, *Geophys. Res. Lett.*, *31*, L12201, doi:10.1029/2004GL019955.

Sejrup, H. P., H. Haflidason, B. I. Hjelstuen, A. Nygard, P. Bryn, and R. Lien (2004), Pleistocene development of the SE Nordic seas margin, *Mar. Geol.*, *213*(1–4), 169–200, doi:10.1016/j.margeo.2004.10.006.

Shackleton, N. (1974), Attainment of isotopic equilibrium between ocean ater and the benthonic foraminiferal genus Uvigerina: Isotopic changes in the ocean during the last glacial, in *Methodes Quantitatives d'Etudes des Variations du Climat au Cours du Pleistocene*, edited by J. Laberyrie, pp. 203–209, Cent. Natl. de la Rech. Sci., Paris.

Shindell, D., D. Rind, N. Balachandran, J. Lean, and P. Lonergan (1999), Solar cycle variability, ozone, and climate, *Science*, *284*(5412), 305–308, doi:10.1126/science.284.5412.305.

Shindell, D. T., G. A. Schmidt, M. E. Mann, D. Rind, and A. Waple (2001), Solar forcing of regional climate change during the maunder minimum, *Science*, *294*(5549), 2149–2152, doi:10.1126/science.1064363.

Skagseth, O., K. A. Orvik, and T. Furevik (2004), Coherent variability of the Norwegian Atlantic slope current derived from TOPEX/ERS altimeter data, *Geophys. Res. Lett.*, *31*, L14304, doi:10.1029/2004GL020057.

Slonosky, V. C., P. D. Jones, and T. D. Davies (2001), Atmospheric circulation and surface temperature in Europe from the 18th century to 1995, *Int. J. Climatol.*, *21*, 63–75, doi:10.1002/joc.591.

Stouffer, R. J. (2004), Time scales of climate response, *J. Clim.*, *17*(1), 209–217, doi:10.1175/1520-0442(2004)017<0209:TSOCR>2.0.CO;2.

Stuiver, M., G. W. Pearson, and T. Braziunas (1986), Radiocarbon age calibration of marine samples back to 9000 cal yr BP, *Radiocarbon*, *28*(2B), 980–1021.

Sutton, R. T., and D. L. R. Hodson (2005), Atlantic Ocean forcing of North American and European summer climate, *Science*, *309*(5731), 115–118, doi:10.1126/science.1109496.

Tung, K. K., and C. D. Camp (2008), Solar cycle warming at the Earth's surface in NCEP and ERA-40 data: A linear discriminant analysis, *J. Geophys. Res.*, *113*, D05114, doi:10.1029/2007JD009164.

Turney, C., M. Baillie, S. Clemens, D. Brown, J. Palmer, J. Pilcher, P. J. Reimer, and H. H. Leuschner (2005), Testing solar forcing of pervasive Holocene climate cycles, *J. Quat. Sci.*, *20*(6), 511–518, doi:10.1002/jqs.927.

Wallace, J. M. (2000), North Atlantic Oscillation/annular mode: Two paradigms-one phenomenon, *Q. J. R. Meteorol. Soc.*, *126*(564), 791–805, doi:10.1256/smsqj.56401.

Weber, S. L. (2005), A timescale analysis of the Northern Hemisphere temperature response to volcanic and solar forcing, *Clim. Past*, *1*, 9–17, doi:10.5194/cp-1-9-2005.

White, W. B., D. R. Cayan, and J. Lean (1998), Global upper ocean heat storage response to radiative forcing from changing solar irradiance and increasing greenhouse gas/aerosol concentrations, *J. Geophys. Res.*, *103*(C10), 21,355–21,366, doi:10.1029/98JC01477.

Woods, T. N., and J. Lean (2007), Anticipating the next decade of sun-earth system variations, *Eos Trans. AGU*, *88*(44), 457–458, doi:10.1029/2007EO440001.

J. T. Andrews and S. J. Lehman, Institute of Arctic and Alpine Research, University of Colorado at Boulder, Boulder, CO 80303, USA. (scott.lehman@colorado.edu)

I. M. Berstad, H. Haflidason, and H. P. Sejrup, Department of Earth Science, University of Bergen, N-5007 Bergen, Norway.

R. Muscheler, GeoBiosphere Science Centre, Lund University, SE-22362 Lund, Sweden.

D. Noone, Cooperative Institute for Research in Environmental Sciences, University of Colorado at Boulder, Boulder, CO 80303, USA.